17th International Mining Congress and Exhibition of Turkey- IMCET2001, ©2001, ISBN 975-395-417-4

Assessment of Open Pit Coal Mining Impacts Using Remote Sensing: A Case Study from Turkey

T.Toren
General Directorate of Turkish Coal Enterprises, Ankara, Turkey
E.Ünal
Department of Mining Engineering, Middle Eos! Technical University, Ankara, Turkey

ABSTRACT: The environmental impacts of coal mining are many and diverse. However, coal is an essential source of energy in meeting the requirements of the existing and growing industries of a *country*. Damage to the environment is usually seen as an unavoidable consequence of maintaining national development It is also desirable to optimize and minimize environmental impacts by adopting proper mining techniques. Therefore, it is necessary to have quickly accessible, cost-effective, multi-temporal information regarding the area's environmental status. Remote sensing technology affords a viable means of analyzing the changing conditions at mine sites. In this study, multi-temporal Landsat TM data sets from the Soma coal basin were subjected to a number of digital image processing techniques to assist in identifying and monitoring the environmental impacts. The application of digital image processing proved to be an effective means of analyzing the multi-temporal data set

1 INTRODUCTION

The environmental impacts of coal mining are many and diverse. Mining operations cause degradation of the land, loss of forest, topsoil and agricultural land, changes in topography and hydrologie conditions, and the pollution of useable surface and ground water. However, coal is an essential source of energy İn meeting the requirements of the existing and growing industries of a country. Damage to the environment is usually seen as an unavoidable consequence of maintaining national development It is also desirable to optimize and minimize environmental impacts by adopting proper mining techniques, rapidly reclaiming the already damaged parts and identifying the areas vulnerable to environmental damage in the near future. All these need quickly accessible, synoptic, cost-effective, multi-temporal information regarding the research area's environmental status (Chatterjee et al. 1994).

Remote sensing technology affords a viable means of analyzing the changing conditions at mine sites. In addition, the information derived from these data provides a means of assessing environmental compliance and can serve as evidence during litigation.

The Soma coal basin, which has been subject to both open pit and underground mining for more than 60 years, was chosen as the "case study area" for the present study. Multi-temporal Landsat TM data sets from the Soma coal basin were subjected to a number of digital image processing techniques to assist İn identifying and monitoring environmental impacts. Smce it was impossible to find geochemical data for the available satellite images, the research only dealt with the topographic and vegetation changes due to mining operations.

2 RESEARCH AREA

The Soma coal basin lies in the province of Manisa in western Turkey. It is 90 km from Manisa city center and 80 km from Balıkesir city center (Figure 1). The average elevation of the basin from sea level İs around 160 m. The coal basin is composed of three main districts, namely, Soma, Deniş, and Eynez. In this study, southern open pit mines of Aegean Lignite Establishment (ELİ), one of the establishments of the state-owned Turkish Coal Enterprises (TKİ), were studied.

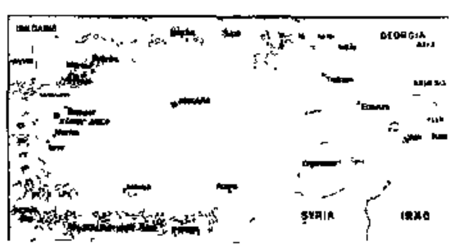

Figure 1. Location of study area

Lignite deposits from the Mesozoic, Tertiary (Miocene and Pliocene) and Quaternary ages are present in the area. Miocene lignite has been mined İn the area since 1939 by ELİ. The total reserve of the area is about 600 million tons, and annually about 10 million tons of lignite is mined from the open pitsofELt.

3 DATA ACQUISITION AND METHODS

3.1 *Preparation of Ancillary Data*

The research area (15.6 km width by 19.8 km length) was determined from six topographic maps of the region (1,000-m Universal Transverse Mercator grid, zone 35, international spheroid, scale 1/25,000, printed in 1978) and then the topographic contour lines of this area were scanned using an A0-sized scanner. Using eight GCPs for each map, six topographic maps were geo-referenced with the projective transformation method that is recommended for scanned materials. To digitize the contour lines, an on-screen digitizing method was used. In this method, a transparent layer is laid over the geo-referenced topographic maps, each topographic contour line is drawn using the mouse, and then the contour value is given. Using this method, 1079 topographic contour lines were digitized with an increment of 10-m contour lines. After the digitizing operation, the minimum contour value of the region was found to be 80 m, whereas the maximum contour value of the region was 1210m.

A digital elevation model (DEM) is a regularly spaced grid covering a surface area, with elevation values associated with each grid location. The DEM, therefore, provides a general model of the earth's surface which becomes more accurate as the distance between grid points decreases. Gridding produces a regularly spaced array of z (e.g., height) values from irregularly spaced xyz data. It does this by extrapolating or interpolating z values at the regularly spaced locations where the data is missing. In this research, using the ERMapper 6.1 software "gridding wizard", me DEM of the region was obtained for 10-m pixel size. To increase the accuracy of the operation, spot heights of the region that are shown on the topographic maps were also digitized and used during the gridding operations.

Any data shown in 2D can also be shown in 3D, provided a suitable height component can be used. A digital terrain model (DTM) of the region was obtained using the ERMapper 6.1 software "3D algorithm". This is shown in Figure 2. In this figure, red is used to indicate high locations, and blue to indicate low locations.

During this research, the drainage network of the region was digitized from the topographic maps. In addition, the geology of the region was obtained from the General Directorate of Turkish Coal Enterprises and scanned using an A4 flatbed scanner. Then the map was geo-referenced and, using the on-screen digitizing method, die geological units and faults of the region were digitized.

Figure 2. DTM (3D view) of the Soma region.

3.2 *Image acquisition and preprocessing*

Landsat Thematic Mapper (TM) images of the area were acquired in the years 1989 and 1999 (path 181, row 33). Atmospheric correction of the Landsat TM images was necessary so that the change detection method employed in this investigation could be used (Singh 1989). During this research, the darkest object subtraction method was used to correct atmospheric effects.

In order to analyze imagery from different dates, the data layers must be spatially co-registered so that the ground measurements and satellite data are in the same spatial reference frame. Image registration was carried out by locating a certain number of ground control points (GCPs) in both images. The latitude and longitude of the GCPs were determined from accurate base maps. The differences between the actual GCP locations and their positions in the image are used to determine the geometric transformations required to restore die image. A nearest-neighbor algorithm was used to resample the corrected images to 30-m pixel size, resulting in a 5.7-m RMS error based on die GCPs.

3.3 *Image enhancement andxlassification*

After preprocessing of the satellite data, several image enhancement methods were applied in order to differentiate die classes. After the visual interpretation of different band combinations, we were able to estimate most of the classes in me region.

RGB321: This algorithm is a natural color scene comprising Landsat TM bands 3, 2, and 1 (approximately equal to red, green, and blue visible light) imaged in the red, green, and blue computer monitor guns respectively. The composite is not totally natural because the Landsat TM bands do not exactly match the red, green, and blue spectral regions; bands 1 (blue visible) and 3 (red visible) have lower spectral ranges Üıan those which the eye recognizes as blue and red. This image looks partly realistic but there is an apparent absence of green vegetation. The "greenness" response of plants is not a very strong one (compare the reflectance of vegetation in the green visible range, 0.56 *p.m.,* Landsat TM band 2), but the human eye is most sensitive to green (it has many more cones sensitive to green) and therefore magnifies the response relative to blue and red. This image combination has lower spatial resolution due to band 1 and has limited spectral diversity since no reflected IR bands are used. Landsat TM RGB321 views of the Soma region (for both 1989 and 1999) are shown in Figure 3.

Figure 3. Landsat TM RGB321 views of the Soma region {1989 on the left, and 1999 on the right).

RGB432: This algorithm is a false color image, usually referred to as standard false color. In this image, Landsat TM band 4 is assigned to the red layer, band 3 (0.66 um, visibİe red) İs in a green layer and band 2 (0.56 um, visible green) in a blue layer. The result of this RGB color composite İs that the high reflectance of vegetation (0.83 u.m, TM band 4) makes vegetation appear red; red features, such as Fe-rich soils appear green, while green features appear blue. This false color image is generally the one used to evaluate a particular image for a variety of resource-based applications. People interested in vegetation can see the location and density of vegetation; people interested in geology can make the same determination - and avoid the over-vegetated images. This algorithm has moderate spatial resolution, whereas it has limited spectral diversity. Landsat TM RGB432 views of the Soma region (for both 1989 and 1999) are shown in Figure 4.

Figure 4. Landsat TM RGB432 views of the Soma region (1989 on the left and 1999 on the right)

RGB74I: This İs a false color image widely used for geological applications. Landsat TM band 7 is assigned to a red layer, band 4 to a green layer and band 1 to a blue layer. The advantage of the RGB741 algorithm is that we achieve better color separation, improving detail and information. A second advantage is that certain mineral groups of interest have distinctive spectral features İn Landsat TM bands 7,4 and 1. In band 1, iron-bearing minerals have low reflectance, whereas phyllosilicates, quartz, and other light-colored minerals have high reflectance. In band 7, phyllosilicates and carbonates have absorption features, whereas hematite and, to a lesser extent, goethite have higher responses. Therefore, the RGB741 composite allows a certain degree of lithological interpretation. Hematite-rich rock and soil is red, quartzites generally appear blue to blue-green because they are light in color and have no iron, while limestones generally appear pale blue or lavender because of the absorption of carbonate in band 7 and their general pale color (high in the blue gun of the computer monitor). Various cements and fracture fillings also add to the spectral responses. Fireburn scars, particularly recent ones, appear red and may be confused with hematite-rich areas. In mis algorithm, coal is generally purple, highly reflective surfaces are white, water is blue, and overburden is gray. Landsat TM RGB741 views of the Soma region (for both 1989 and 1999) are shown İn Figure 5.

Figure 5 Landsat TM RGB741 views of the Soma region (1989 on the left and 1999 on the tight).

RGB view of principal components (PC) 1,2,3: This algorithm generates PCI, PC2, and PC3 and displays them as an RGB image, which is generally used for alteration mapping. The principal component analysis operation is a mathematical method to uncover relationships among many variables and to reduce the amount of data needed to define the relationships. With principal component analysis, each variable (input map) is transformed into a linear combination of orthogonal common components (output maps) with decreasing variation. The linear transformation assumes the components will explain all of the variance in each variable. Hence, each component carries different information that is uncorrelated with other components. Principal component analysis results in linear transformation of a set of (satellite) raster maps into a set of output raster maps, each explaining a common component in the input raster maps. The number of output raster maps is taken as identical to the number of input raster maps so as to enable the user to determine the actual amount of reduction. The output raster maps are listed in decreasing order of variance. This enables the reduction of maps because the last transformed maps have little or no variation left (they may be virtually constant maps), do not add significance to the common components, and may hence be discarded. Principal component analysis can be used for several purposes, e.g., data compression, the preprocessing procedure before classification of the data, and finding targets of interest. It is also possible to generate a PCI, PC2, and PC3 image using only Landsat TM bands 7, 4, 1 of the Landsat TM data. Since these bands show mineralogy, this can be a good image for highlighting geology. RGB view of Principal Components of Landsat TM Bands of 741 (1989) is shown in Figure 6.

Figure 6. RGB view ot Principal Components of Landsat TM Bands of 741(1989).

Landsat TM images over DTM: This operation drapes Landsat TM satellite imagery over DEM data to provide a combined view with height from the DEM and color information from the Landsat TM data. Since Landsat TM has a 30-meter ground resolution per pixel, this type of view is only good for large regional overviews. The research area (for both 1989 and 1999) was modeled in 3D using satellite imagery as shown in Figure 7.

Vegetation NDVI: NDV1 (normalized difference vegetation index) is a commonly used vegetation index that transforms multi-spectral data into a single image band representing vegetation distribution. The NDVI values indicate the amount of green vegetation present in the pixel, where higher NDVI values indicate more green vegetation. NDVI values range from -1 to 1. Vegetated areas will generally yield high values because of their relatively high near-infrared reflectance and low visible reflectance. In contrast, water, clouds, and snow have larger visible reflectance than near-infrared reflectance Thus, these features yield negative index values. Rock and bare soil areas have similar reflectance in the two bands and result in vegetation indices near zero.

In this algorithm, red is used to indicate high NDVI values, and blue to indicate low NDVI values. Figure 8 shows die NDVI views of the Soma region (for both 1989 and 1999).

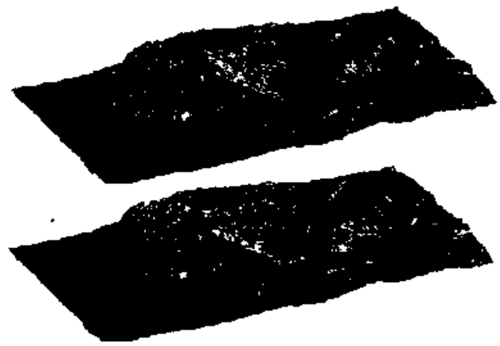

1 igure 7 RÜB542 Landsat TM images of the Soma region over DTM (1989 on the top and 1999 on the bottom)

Figure 8 NDVI views of the Soma region (1989 on ihetopand 1999 on the bottom)

In this figure, it is very easy to see the vegetation changes in the region. The mining area (blue area at the center of the images) changed rapidly over the 10-year period (from 1989 to 1999) and a huge spatial increment occurred in the mining area. In addition to this, an increment was also observed İn regions of high vegetation density (red-colored areas). GPS (Global Positioning System) measurements made during field trips, maps of the Ministry of Forestry and data obtained from the General Directorate of Turkish Coal Enterprises confirmed these changes. During tree plantation works started by the Ministry of Forestry in 1995, approximately 25,000 pine trees were planted in the region, and the General Directorate of Turkish Coal Enterprises planted the landslide and old dumping sites. NDVI maps also showed the increment of the cultivated areas around Bakır Çay. Table 1 shows the classified NDVI values of the Soma region (308.88 km^2).

Table 1 Classified NDVI values of the Soma region.

NDVI		1989	1999	CHANGE
Lower Value	Upper Value	(%)	(%)	(%)
0.8	1.0	0.14	8.62	8 48
06	0.8	7.58	24 30	16 72
04	0.6	21.59	21.31	-0 28
0.2	0.4	26.60	20.75	-5.85
0	02	29 72	17 17	-12 55
• 02	0	12 35	7 75	-4 60
-0.4	-0.2	1.62	006	-1.56
-0.6	-04	0 29	0.02	-0 27
-0 8	-0.6	0.06	0.01	-0 05
-10	-0.8	0.05	0 01	-0.04

As can be seen in the table, during the 10-year period (from 1989 to 1999), vegetated areas (having positive NDVI values) increased about 6.52% (approximately 20 km^2), especially highly vegetated areas (NDVI values greater than 0.6) increased about 25.2% (approximately 78 km^2). These values support the increase in vegetation density and tree plantation works in the region.

Detailed investigations conducted in the field showed that the calculated NDVI clearly depicted areas of dense vegetation. However, the applied index was not successful in separating areas with sparse vegetation. Mining areas are characterized by low levels of vegetation cover. Most of the mining sediments vary İn texture,' oxidation crusts, and coaly particle content. The color differs from light gray through mid and dark gray to black depending on the coal content. A low coal content has a strong influence on the color and therefore on the spectral reflectance. The brightness of the mining sediments has an impact on the vegetation index. In this study, we suspect that this is the reason for the unsatisfactory results. The NDVI values were lower in the open pit mining areas than in the already reclaimed areas, even when both areas had the same type of vegetation and the same percentage cover.

Classification: Unsupervised classification is of maximum utility in classifying images where limited field information İs available for accurate location of training sites or where a large number of spectral classes are present. Where numerous scenes are to be classified with few terrain classes of interest and where field information is available to assist training, a supervised classification is most suitable in mined-land applications (Rathore & Wright, 1993).

In this study, the maximum likelihood method was chosen. This method is the most commonly used supervised classification method (Schmidt & Glaesser, 1998). This algorithm provided the most promising results. The maximum likelihood classification assumes mat spectral values of training pixels are statistically distributed according to a 'multivariate normal probability density function'. For each set of spectral input values, the distance is calculated towards each of the classes. If this distance is smaller than the user-defined threshold value, the class name with the shortest distance is assigned; otherwise, the undefined value is assigned.

During this study, firstly, 30 control points for supervised classification were obtained in the field using Garmin 12-type hand GPS. After inspection of the photographs and camera views recorded during the field trips, using vegetation maps of the region obtained from the Ministry of Forestry, five main classes were determined in the area: mining area, forest, cultivated area, bare soil, and urban settlement. Then, training sites that carry the characteristic features of these classes were defined using the software. Each Landsat TM image had its own training sites. This was necessary because of the high temporal variability of the region.

After the maximum likelihood classifier was applied for several band and data combinations, the results were compared with the ancillary data in order to assess the accuracy. Some classes could not be identified from Landsat TM data when using just some of the bands. Because of the spectral heterogeneity of the surface mine areas coupled with their spatial complexity, the spectral resolution achieved by using selected bands was not enough to classify all mine and reclaimed features with satisfactory accuracy. The use of all Landsat TM bands (except band 6, i.e., the thermal band) gave the best results for all classes together. Land cover maps of the region, for both 1989 and 1999, were created (Figure 9 and Figure 10 respectively).

It was found that computer processing of data by itself was inadequate for accurate determinations of active mine boundaries or areas of coverage. This was primarily due to the fact that a number of other features such as road cuts, construction sites, and agricultural fields produced very similar signatures. Many features of small aerial extent (smaller than a Landsat TM pixel) were not extracted by the classification. Table 2 shows the results of the classification of all classes and their temporal and spatial changes.

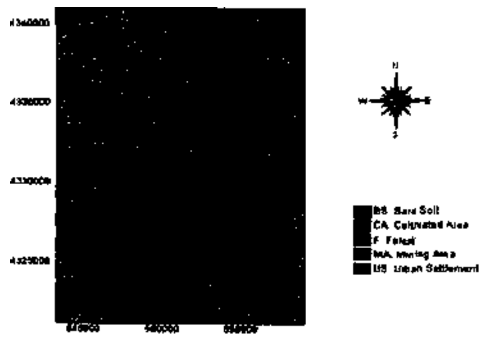

Figure 9. Land cover map of the Soma region (1989).

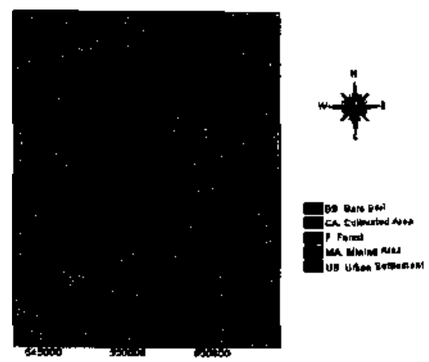

Figure 10. Land cover map of the Soma region (1999)-

Table 2. Results of classification.

CLASS	1989 Area (km²)	1989 Ratio 06)	1999 Area (km-¹)	1999 Ratio (%)	CHANGE Area (km¹)	CHANGE Ratio 1%)
Bare Soil	101.35	33.14	90.85	29.76	-10 50	-3.38
Cultivated	55.43	17.86	18.23	5.87	-37.20	-11.99
Forest	103.33	33.29	120.93	38.96	17 60	5.67
Mining Area	14.70	4.74	41.00	13.21	26 30	8.47
Urban Settlement	34.07	10.97	37.87	12.20	3.80	1.23

As can be seen in the table, mining activities in the region increased about three times in the 10-year period (from 1989 to 1999). During this period, bare soil decreased by about 10.5 km, whereas forest increased about 17.6 km due to the tree plantation work conducted by both the General Directorate of Turkish Coal Enterprises and the Ministry of Forestry. Due to the mining activities and industrial developments in the region, urban settlement also increased. Although it seems from the table that cultivated areas decreased dramaticaHy (by about 11.99 km), the figures show that most of the cultivated areas were changed into forestry.

4 CONCLUSIONS

One of the most obvious and major impacts of surface mining is severe land disruption and degradation. Periodic mapping and monitoring of the aerial extent and location of this degradation can be of vital importance in formulating strategies for reclamation once mining has ceased.

A review of the literature indicates that satellite and aerial remote sensing data have been widely and effectively used to monitor the environmental effects of surface mining activities. There is evidence, however, to suggest that increased spatial resolution of Landsat TM does not necessarily ensure increased classification accuracy, as higher spatial resolution leads to increased spectral variability, which in turn may hinder accurate classification.

Landsat TM and other satellite remote sensing data are useful for the investigation and monitoring of lands devastated by open pit mining activities. The results of this work show the cost- and time-effective opportunities of using high-resolution satellite data for monitoring surface mining and reclamation processes in Turkey. In comparison with conventional data acquisition and interpretation methods, satellite images are a good data source with useful temporal resolution. The spatial complexity and the spectral heterogeneity of the surface mine areas made the application of the satellite data more difficult. However, the main surface mine and reclaimed features were detected and monitored by means of Landsat TM data.

In summary, the potential of satellite remote sensing for monitoring lignite open pit mines is much higher than has been recognized thus far. However, remote sensing will not replace conventional methods entirely. The combination of space-borne and airborne remote sensing and conventional methods will provide a useful and cost effective tool for monitoring devastated lands over a longer period.

REFERENCES

Chatterjee, R.S., Bannerjee, D., Roy, J., & Bhattacharya, A.K. 1994. Landsat TM data processing techniques for identifying and delineating environmental impacts of coal mining. *ITC Journal.* 2:155-162

Rathore, CS. & Wright, R. 1993. Monitoring environmental impacts of surface coal mining. *International Journal of Remote Sensing.* 6:1021-1042

Schmidt, H. & Glaesser, C 1998 Multitemporal analysis of satellite data and their use in the monitoring of the environmental impacts of open cast lignite mining areas in Eastern Germany. *International Journal of Remote Sensing.* 12:2245-2260.

Singh, A. 1989. Digital change detection techniques using remotely sensed data. *International Journal of Remote Sensing* 6:705-715.